Water Science & Technology

IWA PUBLISHING

Water Science & Technology Vol 85 No 1, 52 doi: 10.2166/wst.2021.509

Cephalexin removal by persulfate activation using simulated sunlight and ferrous ions

Carlos M. García Perdomo[a,b], Paula A. Ramírez Minota[a,b], Henry Zúñiga-Benítez[a,b,*] and Gustavo A. Peñuela[a]

[a] Grupo GDCON, Facultad de Ingeniería, Sede de Investigación Universitaria (SIU), Universidad de Antioquia UdeA, Calle 70 # 52-21, Medellín, Colombia
[b] Departamento de Ingeniería Química, Facultad de Ingeniería, Universidad de Antioquia UdeA, Calle 70 # 52-21, Medellín, Colombia
*Corresponding author. E-mail: henry.zuniga@udea.edu.co

ABSTRACT

This study presents the main results related to the use of activated persulfate (PS) in the elimination of the beta-lactam antibiotic cephalexin (CPX). Experiments were done using $K_2S_2O_8$ and simulated sunlight. A face-centered central composite experimental design was used to analyze the effects of the solution pH and the PS concentration on the reaction, and to determine the optimized conditions that favor the CPX elimination. The results indicated that the removal of CPX is promoted by an acidic pH and under the higher evaluated PS dose (7.5 mg L^{-1}). CPX total removal was achieved in 30 min. The analysis of the effect of the pollutant initial concentration indicated that a pseudo-first-order kinetics model can be used to describe the reaction. Likewise, the use of Fe^{2+} ions for PS activation (in the dark) was evaluated and established that a higher concentration of ions favors the pollutant removal. Control tests and under the presence of scavenger agents indicated that both HO• and SO_4^{-}• radicals would be present in the solution and promote the CPX elimination. The assessment of the solution dissolved organic carbon, nitrates and sulfates was also carried out, and indicated that a portion of the organic matter was mineralized.

Key words: advanced oxidation technologies, antibiotics, cephalexin, persulfate activation, sulfate radical anion, water treatment

HIGHLIGHTS

- Antibiotic cephalexin was eliminate using persulfate and simulated sunlight.
- Antibiotic total elimination was achieved in 30 min.
- Ferrous ions can activate persulfate and promote cephalexin removal in water.
- HO• and SO_4^{-}• radicals would be present in the solution.
- Part of the organic matter was mineralized.

INTRODUCTION

Advanced oxidation technologies (AOT) have been used during the last decades in the remediation of different environmental matrices, especially in the elimination of organic pollutants from aqueous matrices at laboratory and pilot plant scale (Lado Ribeiro *et al.* 2019; Chen *et al.* 2021). These technologies are based on the generation of highly reactive species, including the hydroxyl radical (HO•), capable of oxidizing practically any organic pollutant present in water. HO• can be generated through different physicochemical reactions whose efficiency depends on operational parameters such as the solution pH, the concentration and nature of the target pollutants, the presence or absence of light radiation (UV or solar), etc. (Vieira *et al.* 2021). However, there are other radical species that also have the potential to eliminate organic compounds from water, as is the case of the sulfate radical anion SO_4^{-}• (Chen *et al.* 2021).

SO_4^{-}• are radicals that have proven their power in degrading organic pollutants such as pharmaceuticals and antibiotics (Ushani *et al.* 2020). SO_4^{-}• has a higher redox potential and a longer half-life in comparison to HO• (Amor *et al.* 2021), and can be generated from persulfate ($S_2O_8^{2-}$, PS) activation either thermally, mediated by light radiation, or by interaction with transition metals (such as ferrous ions, Fe^{2+}). Equation (1) presents the PS activation via light radiation, in which the $S_2O_8^{2-}$ bonds are broken generating SO_4^{-}•. The energy required to break the O–O bond of $S_2O_8^{2-}$ is 120 kJ mol^{-1}, thus electromagnetic energy with wavelength <500 nm would be adequate for this purpose (Ushani *et al.* 2020). In the activation with Fe^{2+} (Equation (2)), ferrous ions are transformed into Fe^{3+} while $S_2O_8^{2-}$ generates SO_4^{-}• and SO_4^{2-} (Yang *et al.* 2019; Amor *et al.* 2021; Yan *et al.* 2021). In addition, SO_4^{-}• can be transformed to HO• in aqueous solutions according to Equation (3) (Yang *et al.* 2019). Among the advantages of these methods are their low cost and easy implementation compared to

other AOTs. However, its performance can be affected by the pH of the solution, and the concentrations of the precursor salt (source of $S_2O_8^{2-}$) and the Fe^{2+} ions (Ushani *et al.* 2020; Amor *et al.* 2021):

$$S_2O_8^{2-} + hv \rightarrow 2SO_4^{-}\bullet \quad (1)$$

$$S_2O_8^{2-} + Fe^{2+} \rightarrow Fe^{3+} + SO_4^{-}\bullet + SO_4^{2-} \quad (2)$$

$$SO_4^{-}\bullet + H_2O \rightarrow SO_4^{2-} + HO\bullet + H^+ \quad (3)$$

Antibiotics are a group of drugs widely used in the treatment of various bacterial infections in human therapy, livestock production, and aquaculture (Gou *et al.* 2021). However, the extensive and widespread use of antibiotics has generated serious ecological and environmental problems related to the ubiquitous presence of their residues in the environment. In this way, the presence of antibiotics has been evidenced in surface waters, in seawater and in wastewater (Gou *et al.* 2021; Yu *et al.* 2021), which could be related to the fact that animals and humans excrete between 10.0 and 90.0% of ingested antibiotics as the parent compounds or its metabolites through urine and feces. In this way, one of the main concerns associated with the presence of antibiotics in different environmental matrices is the proliferation of a variety of genes resistant to antibiotics (bacterial resistance), which could affect the therapeutic efficacy, representing a threat to human and animal health (Yu *et al.* 2021).

Cephalexin (CPX, $C_{16}H_{17}N_3O_4S$, Figure 1) is a beta-lactam cephalosporin antibiotic commonly prescribed for the treatment of skin and soft tissue infections, and uncomplicated urinary tract infections, among others (Everts *et al.* 2021). Its wide range of bacterial activity and high solubility in water make it one of the most prescribed antibiotics worldwide (Tavasol *et al.* 2021). However, the chemical structure and antibacterial nature of CPX limit the use of conventional treatments for its elimination from water (Yu *et al.* 2021). In this way, CPX concentrations of up to 64 μg L^{-1} have been reported in wastewater (Gou *et al.* 2021), and its presence in seawater samples and in coastal sediments has also been informed, which implies that it is necessary to implement new alternatives in the treatment of water containing this antibiotic (Tavasol *et al.* 2021).

Different methods have been used to remove CPX from aqueous solutions including adsorption, ozonation, photo-catalysis, Fenton and related reactions, and catalytic wet peroxide oxidation (Cárdenas Sierra *et al.* 2020; Tavasol *et al.* 2020, 2021; Basturk *et al.* 2021; Gou *et al.* 2021; Yu *et al.* 2021). However, much information regarding the use of activated persulfate on CPX elimination is yet to be reported. Some authors have studied the elimination of CPX using the activation of persulfate thermally and under radiation with low-pressure mercury vapor lamps (Qian *et al.* 2018; Almasi *et al.* 2020; Song *et al.* 2021). In this sense, the objective of this research was to evaluate the application of persulfate activated by simulated sunlight (wavelength 290–800 nm) and ferrous ions in the removal of CPX at the laboratory scale. The use of sunlight would allow the treatment to be carried out in a more economical way compared to processes that require additional energy (heat/temperature) for activation or light with a shorter wavelength. The effects of operational parameters, such as the pH of the solution, the concentration of $S_2O_8^{2-}$, Fe^{2+} and CPX on the reaction, were evaluated. To complement the study, additional tests were carried out to determine the role of HO• and SO_4^{-}• radicals in the pollutant elimination, as well as the determination of the dissolved organic carbon (DOC) and the presence of nitrates (NO_3^{-}) and sulfates (SO_4^{2-}) in the solution.

MATERIALS AND METHODS

Materials

All the used reagents were of analytical grade and, in most cases, were employed as received. CPX (CAS 15686-71-2, purity >98.0%) was obtained from AK Scientific. Potassium persulfate ($K_2S_2O_8$, CAS 7727-21-1, Supelco-Merck) and ferrous sulfate

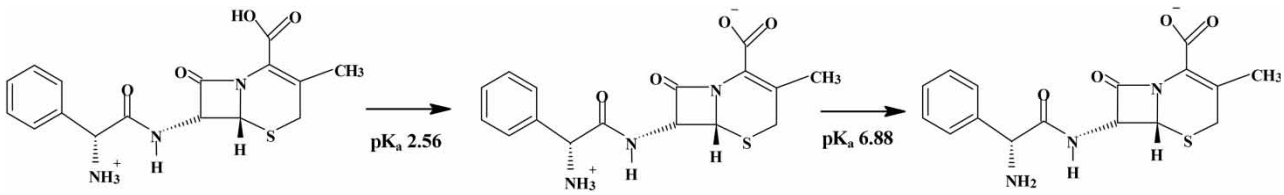

Figure 1 | Chemical structure of cephalexin and its ionization states.

heptahydrate ($FeSO_4 \cdot 7H_2O$, CAS 7782-63-0, Sigma-Aldrich) were used as sources of $S_2O_8^{2-}$ and Fe^{2+} ions, respectively. All solutions were prepared in deionized water and the pH was adjusted using concentrated solutions of NaOH and HCl (Alfa-Aesar).

Ethanol (C_2H_5OH, CAS 64-17-5, AppliChem) and tert-butanol (C_4H_9OH, CAS 75-65-0, Merck) were used to determine the role of HO• and SO_4^{-}• radicals in the contaminant elimination; and high-performance liquid chromatography (HPLC) grade acetonitrile (CH_3CN, 75-05-8, Merck) and formic acid (CH_2O_2, CAS 64-18-6, Merck) were used in the chromatographic analysis.

Persulfate activation using simulated sunlight

Experiments involving the PS activation by simulated sunlight were performed using a photosimulator (Suntest CPS +, Atlas) capable of emitting light with a spectrum like that of the sun (wavelength: 290–800 nm). The amount of the incident light on the solution was set at 500 W m^{-2}. In most of the experiments, 50.0 mL of solution containing 2.0 mg L^{-1} of CPX were treated.

The effects of the solution pH and the $K_2S_2O_8$ concentration in the elimination of CPX were evaluated, considering some preliminary scanning-type experiments in which levels corresponding to acidic, neutral, and basic pH, and persulfate concentrations between 2.5 and 10.0 mg L^{-1} were assessed. Selection of the conditions that lead to a higher CPX removal was carried out using a face-centered central composite experimental design. For each evaluated factor, three levels were selected considering the results of the preliminary tests. The response variable was the extent of CPX removal after 30 min.

The results of the experimental design were analyzed using the Statgraphics Centurion XVI software which allowed determination of the conditions under the evaluated experimental range and that lead to a higher pollutant elimination. Once the optimized conditions were selected, experiments were carried out for 60 min to establish the reaction kinetics and the role of the radical species. In addition, some control tests, such as hydrolysis, photolysis and darkness oxidation with PS, were done.

Finally, the effect of the CPX initial concentration was evaluated, considering the optimized conditions of pH and PS, in the range 1.0–5.0 mg L^{-1}.

All the experiments were done in triplicate and at room temperature (25.0 °C).

Persulfate activation using Fe^{2+}

PS activation using Fe^{2+} ions was carried out considering the $K_2S_2O_8$ concentration optimized in the tests under simulated sunlight. Five concentrations of $FeSO_4$ were evaluated in the elimination of CPX. Experiments were done in the dark, with constant stirring, and for a reaction time of 30 min. The reaction volume was 50.0 mL and the antibiotic concentration was 2.0 mg L^{-1}.

Analytical methods

Samples were drawn at different time intervals. For the experiments with simulated sunlight, 1.0 mL of the solution was taken for analysis, while in the experiments with ferrous ions, 0.25 mL of ethanol was added to 0.75 mL of solution after extraction to stop the reaction (ethanol is capable of scavenging HO• and SO_4^{-}• radicals).

CPX concentration was monitored using HPLC on an Agilent 1100–1200 series system equipped with a diode array detector (DAD) set to 261.4 nm, and a Kinetex C18 column (silica 100 Å pore diameter, 2.5 μm, 4.6 × 150 mm). The eluent was a mixture of acetonitrile/water (0.1% v/v formic acid) in gradient mode (10/90 for 4 min, then 70/30 for 1 min, and finally 90:10 for 4 min) at a flow rate of 0.55 mL min^{-1}. The injection volume was 50 μL and the retention time for CPX was ~6.0 min.

Conversely, the complete oxidation of CPX would lead to the transformation of the organic carbon into CO_2 (mineralization) and to the formation of NO_3^- and SO_4^{2-} (which can also be present in the solution due to reactions with persulfate). In this sense, samples DOC, NO_3^- and SO_4^{2-} concentrations were evaluated following methods 5310B (high combustion temperature method) and 4110B (ion chromatography with chemical suppression of effluent conductivity) proposed previously (Standard Methods for the Examination of Water & Wastewater 2017). More information regarding the analytical methodology can be found in the authors' previous publication (Cárdenas Sierra *et al.* 2020).

RESULTS AND DISCUSION

CPX removal by persulfate activation using simulated sunlight

Optimization of reaction conditions

The pH of the solution and the concentration of $K_2S_2O_8$ are two of the operational parameters with a high influence on the removal of organic pollutants using technologies based on the generation of $SO_4^{-}\bullet$ radicals (Amor *et al.* 2019; Yang *et al.* 2019; Hadi *et al.* 2021). The application of PS and simulated sunlight in the removal of CPX was initially evaluated by conducting exploratory experiments at pH 3.0, 6.0, and 9.0, under an initial contaminant concentration of 2.0 mg L^{-1}, and $K_2S_2O_8$ concentrations of 2.5, 7.5, and 10.0 mg L^{-1}. The results (data not shown) indicated that after 30 min of reaction, a ~92.0% of CPX extent of elimination could be achieved under pH 3.0 and an initial $K_2S_2O_8$ concentration of 5.0 mg L^{-1}. In this way, the optimization of the reaction conditions was carried out using a face-centered central composite experimental design evaluating three experimental levels (low, medium, and high) for each parameter, as is shown by Table 1. The total number of experiments was 11 and the response variable was the percentage of CPX removal after 30 min.

Table 2 presents the results associated with the experimental design. Tests were carried out randomly. Additionally, Figure 2 corresponds to the response surface obtained after the statistical analysis of the data. This figure indicates that it is feasible to achieve a 100.0% CPX elimination within the evaluated experimental ranges. Likewise, Figure 3 corresponds to the main effects plot, from which it can be inferred that increasing, in the evaluated range, the concentration of $K_2S_2O_8$ favors the elimination of CPX, which would be associated with a higher generation of radicals product of the $S_2O_8^{2-}$ ion breakdown by the light radiation (Equation (1)). However, it has been reported that excesses in the concentration of PS can cause a negative effect on pollutant degradation due to its scavenging effects on the radicals, as is indicated by Equations (4) and (5) (Wojnárovits & Takács 2019; Yang *et al.* 2019):

$$S_2O_8^{2-} + HO\bullet \rightarrow S_2O_8^{-}\bullet + OH^{-} \quad (4)$$

$$S_2O_8^{2-} + SO_4^{-}\bullet \rightarrow S_2O_8^{-}\bullet + SO_4^{2-} \quad (5)$$

Table 1 | Experimental levels evaluated in the CPX removal using PS and simulated sunlight

	Level		
Parameter	**Low**	**Medium**	**High**
$K_2S_2O_8$ initial concentration (mg L^{-1})	2.5	5.0	7.5
pH	3.0	6.0	9.0

Table 2 | Experimental design for CPX removal using PS and simulated sunlight (CPX initial concentration 2.0 mg L^{-1}, reaction time 30 min)

Experiment	$K_2S_2O_8$ initial concentration (mg L^{-1})	pH	CPX removal (%) experimental	CPX removal (%) predicted by model
1	5.0	6.0	15.6	18.5
2	2.5	6.0	11.5	16.7
3	2.5	9.0	4.1	1.8
4	2.5	3.0	90.4	87.5
5	5.0	3.0	93.5	89.9
6	7.5	3.0	100.0	100.0[a]
7	5.0	6.0	15.9	18.5
8	5.0	9.0	7.9	3.1
9	5.0	6.0	15.6	18.5
10	7.5	6.0	48.2	34.6
11	7.5	9.0	11.7	18.8

[a]Adjusted value.

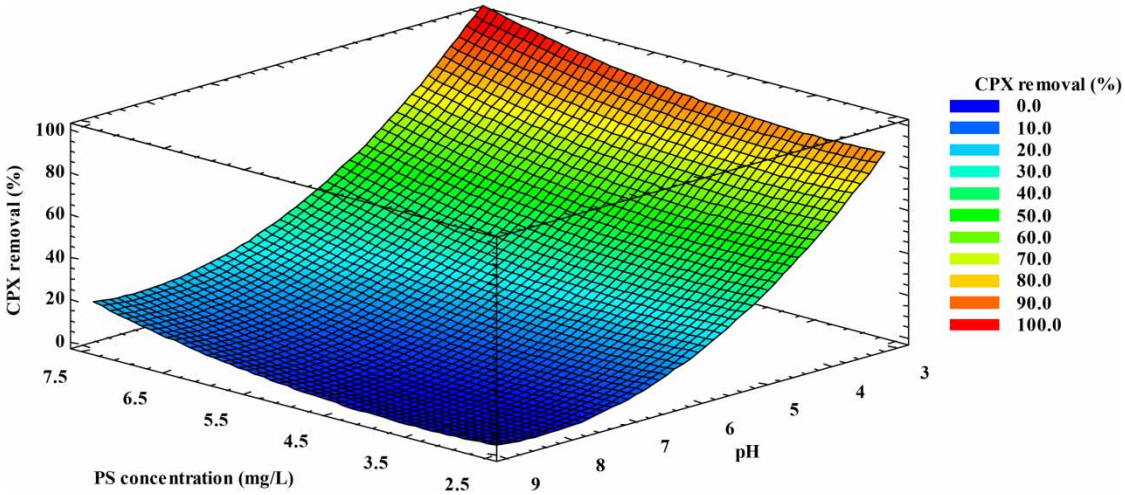

Figure 2 | Response surface for CPX removal using PS and simulated sunlight (CPX initial concentration 2.0 mg L^{-1}, reaction time 30 min).

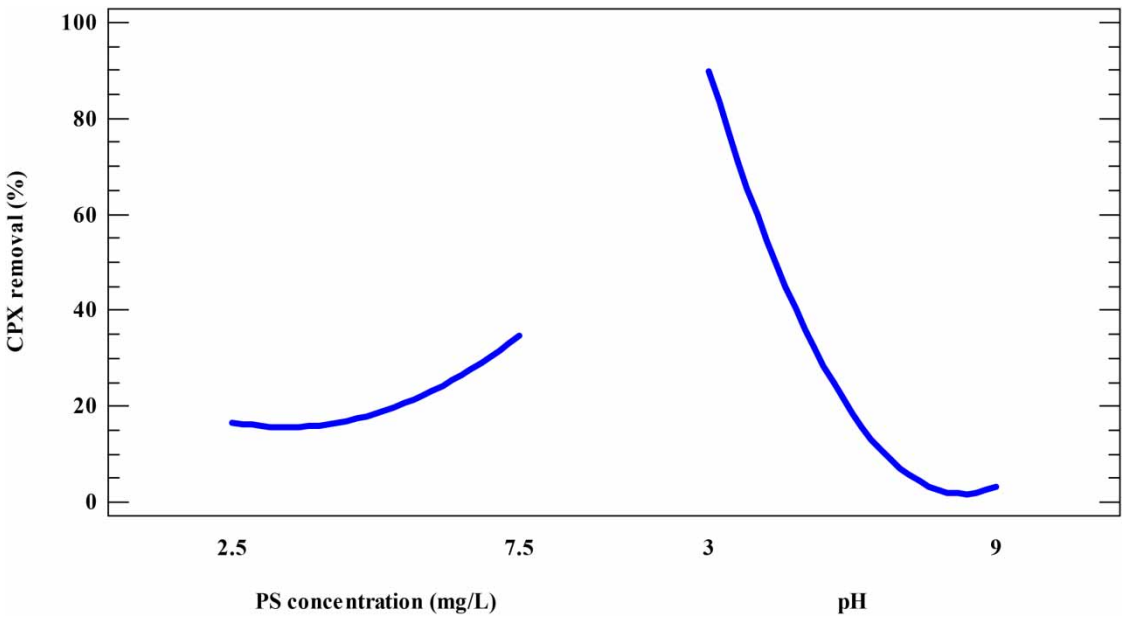

Figure 3 | Main effects plot for CPX removal using PS and simulated sunlight (CPX initial concentration 2.0 mg L^{-1}, reaction time 30 min).

In terms of the effect of the solution pH, Figure 3 indicates that acidic conditions favor the elimination of CPX. This may be due to two reasons: (i) under acidic conditions, the decomposition of $S_2O_8^{2-}$ into radicals is favored (Equations (6) and (7)) (Rajaei *et al.* 2021); and (ii) CPX has two acid dissociation constants (pK_a), one at pH ~2.56 and the other at pH ~6.88 (Legnoverde *et al.* 2014), which implies that at solution pH in the range 2.56 to 6.88 the charge of the CPX molecule would be neutral (isoelectric point ~4.5) (Figure 1) while at more acidic conditions it would be in cationic form and its reactivity would be higher promoting its elimination.

$$S_2O_8^{2-} + H^+ \rightarrow HS_2O_8^- \quad (6)$$

$$HS_2O_8^- \rightarrow SO_4^- \bullet + SO_4^{2-} + H^+ \quad (7)$$

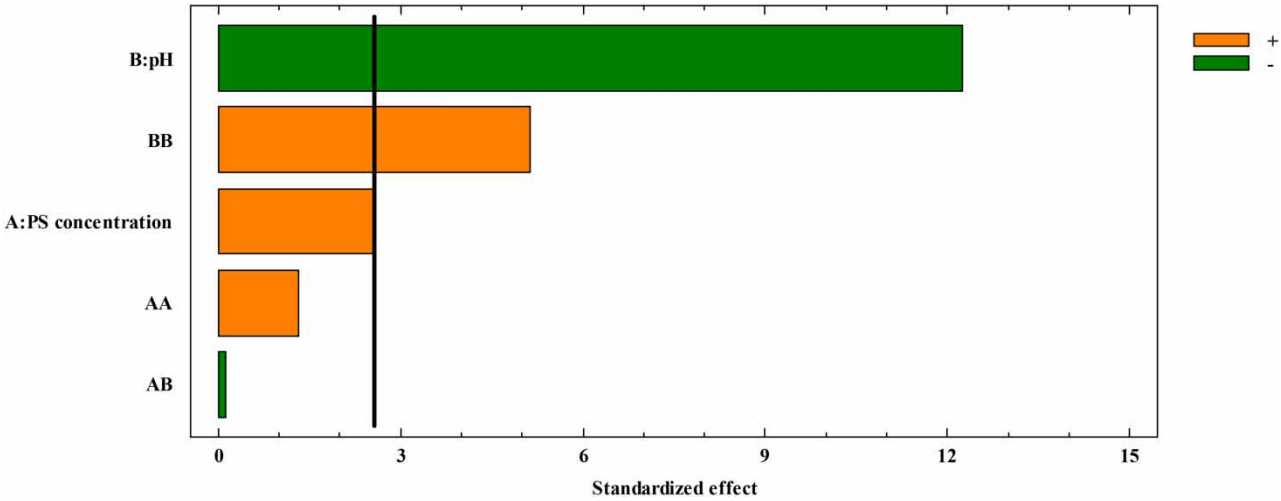

Figure 4 | Standardized Pareto chart for CPX removal using PS and simulated sunlight (CPX initial concentration 2.0 mg L^{-1}, reaction time 30 min).

Figure 4 corresponds to the standardized Pareto chart, and allows establishment of the effect of each parameter on the response variable. According to the figure, pH is the factor with most effect on the reaction, and it was confirmed that higher pH levels inhibit the elimination of CPX (negative effect).

Equation (8) corresponds to the polynomial model that relates the response variable with the factors and interactions analyzed. Additionally, Table 2 presents the values predicted by the model, and Table 3 shows the corresponding data of the analysis of variance (ANOVA) for CPX removal and the determination coefficients for model:

$$\text{CPX removal}\,(\%) = 225.867 - 7.447 * \text{PS} - 51.456 * \text{pH} + 1.144 * \text{PS}^2 - 0.067 * \text{PS} * \text{pH} + 3.111 * \text{pH}^2 \quad (8)$$

where PS is the $K_2S_2O_8$ initial concentration (mg L^{-1}).

Finally, according to the previous description, the conditions that, within the evaluated experimental ranges, led to a higher elimination of CPX (optimized conditions) are pH 3.0 and 7.5 mg L^{-1} $K_2S_2O_8$ initial concentration (predicted CPX removal according to the model: 100.0%).

Table 3 | Analysis of variance for CPX removal and determination coefficients for model

Source	Sum of squares	Degrees of freedom (d.f.)	Mean square	F-ratio	*P*-value
A:PS concentration	484.202	1	484.202	6.44	0.0520
B:pH	11,284.0	1	11,284.0	150.07	0.0001
AA	129.51	1	129.51	1.72	0.2464
AB	1.0	1	1.0	0.01	0.9127
BB	1,986.13	1	1,986.13	26.42	0.0036
Total error	375.947	5	75.1893		
Total (corrected)	14,714.0	10			

R-squared = 97.445%.
R-squared (adjusted by d.f.) = 94.8899%.
Standard error of estimate = 8.67118.
Mean absolute error = 4.93333.
Durbin-Watson statistic = 2.63235 (*P* = 0.6973).
Lag 1 residual autocorrelation = −0.393776.

CPX removal under optimized conditions

The elimination of CPX using PS and simulated sunlight was carried out considering the optimized conditions for solution pH and $K_2S_2O_8$ initial concentration. Figure 5 presents the experimental results, which indicated that after 30.0 min of treatment it was possible to eliminate the contaminant, confirming that the selected conditions are appropriate. In addition, additional experiments were conducted to determine the individual effects of some of the species present in the solution, and possible synergistic effects. In this sense, according to Figure 5, the removal of CPX using hydrolysis, photolysis, and oxidation with $S_2O_8^{2-}$ in darkness was less than 20.0% after 60 min, which indicates that the combined action of $S_2O_8^{2-}$ and sunlight is necessary to achieve a significant removal of the antibiotic. $S_2O_8^{2-}$ anion is a strong oxidant, but at room temperature is not effective enough for organic pollutant elimination when it is used on its own (Wojnárovits & Takács 2019; Hadi *et al.* 2021).

To better understand the degradation mechanism and identify the role of the HO• and SO_4^{-}• radicals formed during the CPX removal using PS and simulated sunlight, ethanol (EtOH) and tert-butanol (TBA) were used to act as radical scavengers. EtOH can react rapidly with HO• and SO_4^{-}•, and TBA has high reactivity with HO• but poor reactivity with SO_4^{-}• (Feng *et al.* 2017; Yan *et al.* 2021). In this sense, according to Figure 6, the removal of CPX in the presence of TBA was ~12.87% after 30 min of reaction, while with the addition of EtOH it was only ~5.82%. In this way, it could be inferred that both radicals would be present in the solution. The lower inhibition shown by TBA is due to its low reaction with SO_4^{-}•, but the role of the HO• radical would be more prominent as under the presence of both scavengers the inhibition was quite marked.

CPX degradation kinetics: effect of pollutant initial concentration

The effect of the CPX initial concentration was evaluated in the range 1.0–5.0 mg L^{-1} using the optimized conditions. In this way, Figure 7 indicates that the obtained extents of removal were higher than ~88.0% after 30.0 min of reaction. Additionally, it was observed that increasing the pollutant concentration reduces its extent of elimination, which indicates that the reaction is dependent on CPX initial concentration. When the antibiotic concentration is higher, the extent of removal is reduced as the proportion of contaminant with respect to the number of radicals present in the solution increases. That is, the number of radicals (HO• or SO_4^{-}•) is the same as that needed to attack a higher amount of CPX. In addition, the generated byproduct concentration would also increase, representing a higher competition to react with the oxidizing species.

Authors have indicated that a pseudo-first-order kinetics model (Equation (9)) can be used to describe the organic pollutants rate of degradation under the use of different TAOs, including those based on PS activation (Pirsaheb *et al.* 2020; Duan *et al.* 2021; Hadi *et al.* 2021). The inset graph in Figure 8 presents the results obtained after evaluating the relationship between the initial reaction rate and the initial CPX concentration and evidenced that, in effect, the proposed model fits the

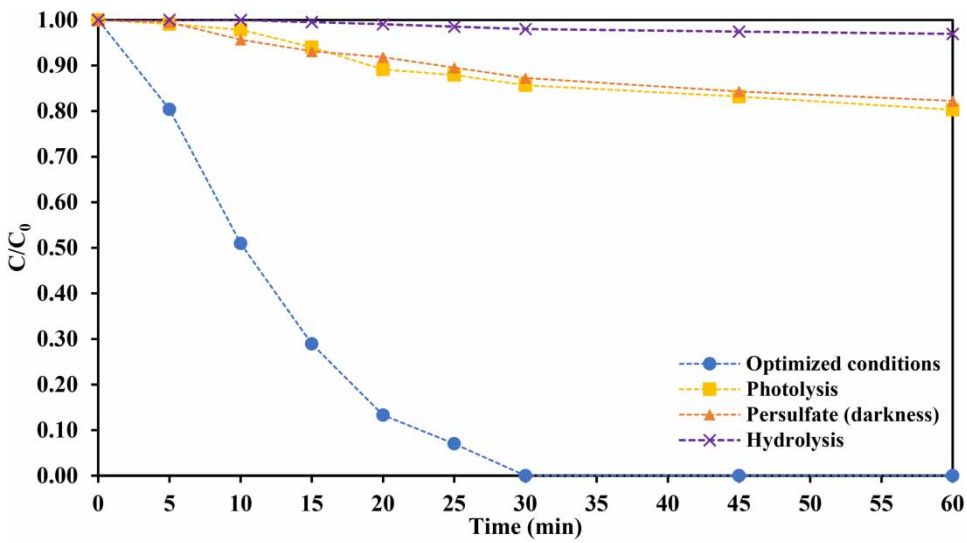

Figure 5 | CPX removal using PS and simulated sunlight under optimized conditions (CPX initial concentration 2.0 mg L^{-1}, pH 3.0, $K_2S_2O_8$ initial concentration 7.5 mg L^{-1}).

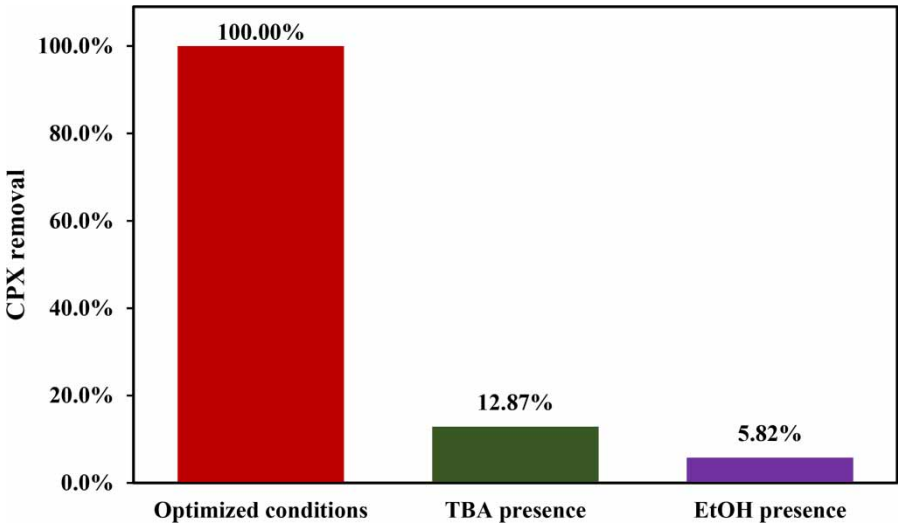

Figure 6 | Effect of scavengers on CPX removal using PS and simulated sunlight (CPX initial concentration 2.0 mg L^{-1}, pH 3.0, $K_2S_2O_8$ initial concentration 7.5 mg L^{-1}, scavengers concentration 200.0 mg L^{-1}, reaction time 30.0 min).

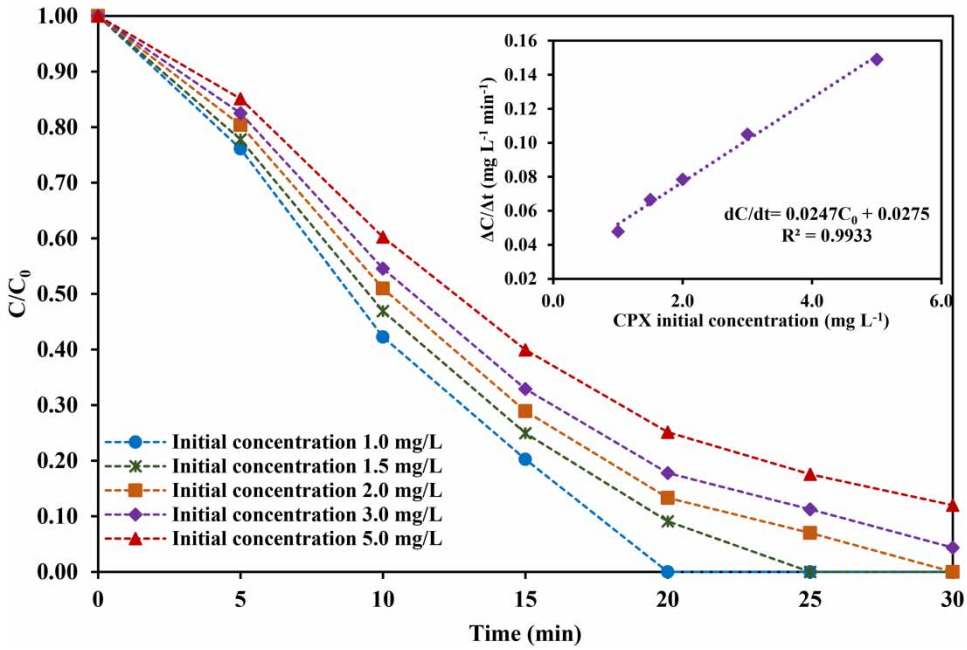

Figure 7 | Effect of CPX initial concentration on its removal using PS and simulated sunlight. Inset graph pseudo-first-order kinetics model assessment (pH 3.0, $K_2S_2O_8$ initial concentration 7.5 mg L^{-1}).

experimental data (R^2 0.9933) with an 0.0247 min^{-1} reaction rate constant:

$$\frac{dC}{dt} \approx \frac{\Delta C}{\Delta t} \approx kC_0 \tag{9}$$

C_0 is the pollutant initial concentration at the time t and k is the reaction rate constant.

CPX removal by persulfate activation using ferrous ions

The activation of PS using Fe^{2+} ions was carried out considering the concentration of $K_2S_2O_8$ optimized in the experiments with simulated sunlight. In this way, according to Equation (2), 7.5 mg L^{-1} of $K_2S_2O_8$ required ~4.5 mg L^{-1} of $FeSO_4$. Tests

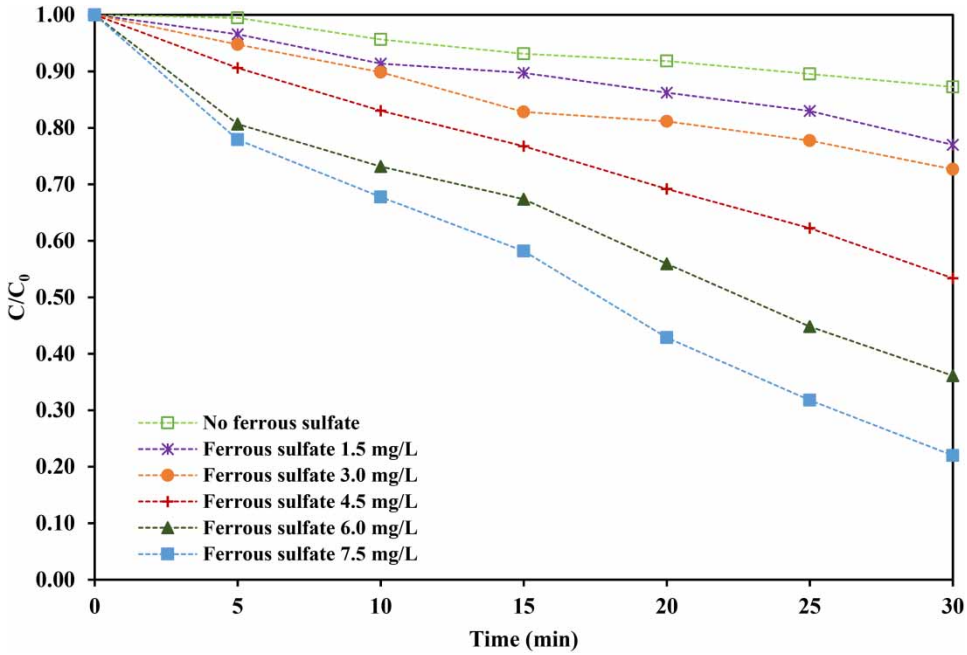

Figure 8 | Effect of Fe^{2+} presence on CPX removal using PS (CPX initial concentration 2.0 mg L^{-1}, pH 3.0, $K_2S_2O_8$ initial concentration 7.5 mg L^{-1}).

were done considering concentrations lower and higher than this value. The pH of the solution was 3.0 and the reaction was conducted in the dark. Figure 8 depicts the obtained results, which indicate that increasing the presence of Fe^{2+} favors the elimination of CPX, reaching a ~78.0% removal in 30 min. However, increasing the dose of Fe^{2+} could have a negative effect, as it can trap both HO• and SO_4^-• radicals as is indicated by Equations (10) and (11) (Wang *et al.* 2019; Yan *et al.* 2021). Furthermore, in terms of applying this type of treatments at pilot or real scale, higher doses of Fe^{2+} would require more post-treatment stages before the final discharge of the treated water, consequently it is not advisable to evaluate higher levels of this parameter:

$$SO_4^-\bullet + Fe^{2+} \rightarrow Fe^{3+} + SO_4^{2-} \quad (10)$$

$$HO\bullet + Fe^{2+} \rightarrow Fe^{3+} + OH^- \quad (11)$$

Evaluation of mineralization and ions presence

The complete oxidation of CPX would lead to the formation of CO_2, NO_3^- and SO_4^{2-}. In this way, to evaluate the variation of the solution DOC and the content of nitrates and sulfates would allow the establishment of the achieved degree of mineralization. Thus, Figure 9 indicates that after 120 min of phototreatment using PS and simulated sunlight (under optimized conditions) only an ~18.0% reduction in the DOC was reached, which contrasts with a significant increase in NO_3^- and SO_4^{2-}concentrations (compared to the initial solutions). The higher presence of NO_3^- is associated with the decomposition of CPX (two nitrogen atoms in the molecule), and the increase in SO_4^{2-} would be due to the oxidation of CPX and its generation from the persulfate decomposition.

The low reduction of DOC would imply that the degradation of CPX leads to the formation of organic byproducts with a higher resistance to oxidation by radicals.

CONCLUSIONS

According to the results of this study, the use of PS and simulated sunlight promotes the complete elimination of CPX in water. The antibiotic removal is favored at acidic pH conditions, and under the evaluated experimental range, at higher concentrations of PS. pH has a more significant effect than persulfate concentration. Furthermore, the removal of the pollutant

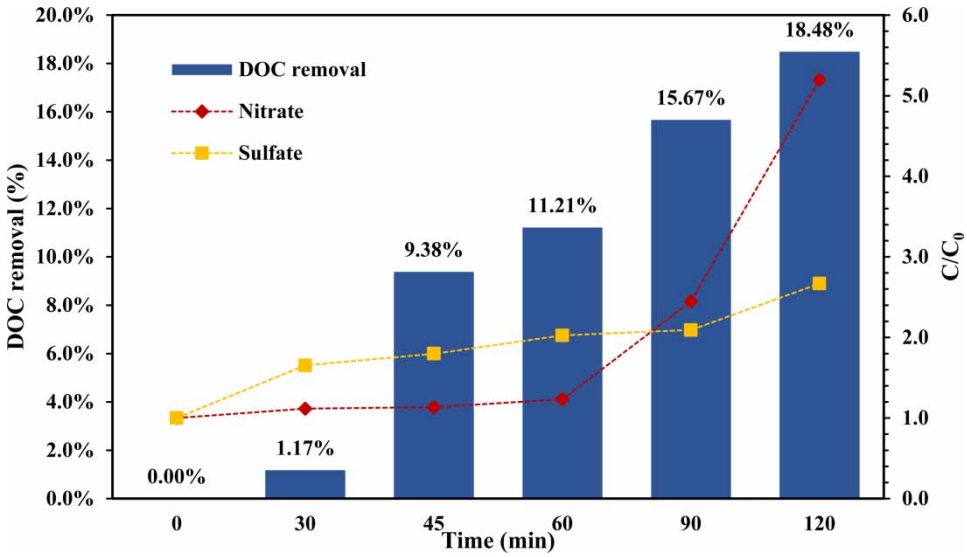

Figure 9 | DOC and ions presence on CPX removal using PS and simulated sunlight (CPX initial concentration 2.0 mg L^{-1}, pH 3.0, $K_2S_2O_8$ initial concentration 7.5 mg L^{-1}).

satisfies a pseudo-first-order kinetics model. The HO• and SO_4^{-}• radicals promote the oxidation of the molecule, whereas the individual effect of photolysis, hydrolysis and $S_2O_8^{2-}$ is lower.

The activation of PS by Fe^{2+} also allows elimination of CPX, but it is important to establish reaction conditions that do not imply the use of an excess of ferrous ions.

Finally, in terms of mineralization, the used treatment is able to remove a portion of the organic matter content in the solutions.

ACKNOWLEDGEMENTS

Authors thank the 'Fundación para la promoción de la Investigación y la Tecnología (FPIT)' of the Colombia Bank of the Republic, and the Universidad de Antioquia for their financial and technical support.

DATA AVAILABILITY STATEMENT

All relevant data are included in the paper or its Supplementary Information.

REFERENCES

Almasi, A., Esmaeilpoor, R., Hoseini, H., Abtin, V. & Mohammadi, M. 2020 Photocatalytic degradation of cephalexin by UV activated persulfate and Fenton in synthetic wastewater: optimization, kinetic study, reaction pathway and intermediate products. *Journal of Environmental Health Science and Engineering* **18** (2), 1359–1373.

Amor, C., Rodríguez-Chueca, J., Fernandes, J. L., Domínguez, J. R., Lucas, M. S. & Peres, J. A. 2019 Winery wastewater treatment by sulphate radical based-advanced oxidation processes (SR-AOP): thermally vs UV-assisted persulphate activation. *Process Safety and Environmental Protection* **122**, 94–101.

Amor, C., Fernandes, J. R., Lucas, M. S. & Peres, J. A. 2021 Hydroxyl and sulfate radical advanced oxidation processes: application to an agro-industrial wastewater. *Environmental Technology & Innovation* **21**, 101183.

APHA 2017 *Standard Methods for the Examination of Water and Wastewater*. American Public Health Association, Washington, DC.

Basturk, I., Varank, G., Murat-Hocaoglu, S., Yazici-Guvenc, S., Can-Güven, E., Oktem-Olgun, E. E. & Canli, O. 2021 Simultaneous degradation of cephalexin, ciprofloxacin, and clarithromycin from medical laboratory wastewater by electro-Fenton process. *Journal of Environmental Chemical Engineering* **9** (1), 104666.

Cárdenas Sierra, R. S., Zúñiga-Benítez, H. & Peñuela, G. A. 2020 Experimental data on antibiotic cephalexin removal using hydrogen peroxide and simulated sunlight radiation at lab scale: effects of pH and H_2O_2. *Data in Brief* **30**, 105437.

Chen, Y. d., Duan, X., Zhou, X., Wang, R., Wang, S., Ren, N. q. & Ho, S. H. 2021 Advanced oxidation processes for water disinfection: features, mechanisms and prospects. *Chemical Engineering Journal* **409**, 128207.

Duan, P., Liu, X., Liu, B., Akram, M., Li, Y., Pan, J., Yue, Q., Gao, B. & Xu, X. 2021 Effect of phosphate on peroxymonosulfate activation: accelerating generation of sulfate radical and underlying mechanism. *Applied Catalysis B: Environmental* **298**, 120532.

Everts, R. J., Gardiner, S. J., Zhang, M., Begg, R., Chambers, S. T., Turnidge, J. & Begg, E. J. 2021 Probenecid effects on cephalexin pharmacokinetics and pharmacodynamics in healthy volunteers. *Journal of Infection* **83** (2), 182–189.

Feng, Y., Song, Q., Lv, W. & Liu, G. 2017 Degradation of ketoprofen by sulfate radical-based advanced oxidation processes: kinetics, mechanisms, and effects of natural water matrices. *Chemosphere* **189**, 643–651.

Gou, Y., Peng, L., Xu, H., Li, S., Liu, C., Wu, X., Song, S., Yang, C., Song, K. & Xu, Y. 2021 Insights into the degradation mechanisms and pathways of cephalexin during homogeneous and heterogeneous photo-Fenton processes. *Chemosphere* **285**, 131417.

Hadi, S., Taheri, E., Amin, M. M., Fatehizadeh, A. & Aminabhavi, T. M. 2021 Advanced oxidation of 4-chlorophenol via combined pulsed light and sulfate radicals methods: effect of co-existing anions. *Journal of Environmental Management* **291**, 112595.

Lado Ribeiro, A. R., Moreira, N. F. F., Li Puma, G. & Silva, A. M. T. 2019 Impact of water matrix on the removal of micropollutants by advanced oxidation technologies. *Chemical Engineering Journal* **363**, 155–173.

Legnoverde, M. S., Simonetti, S. & Basaldella, E. I. 2014 Influence of pH on cephalexin adsorption onto SBA-15 mesoporous silica: theoretical and experimental study. *Applied Surface Science* **300**, 37–42.

Pirsaheb, M., Hossaini, H. & Janjani, H. 2020 Reclamation of hospital secondary treatment effluent by sulfate radicals based–advanced oxidation processes (SR-AOPs) for removal of antibiotics. *Microchemical Journal* **153**, 104430.

Qian, Y., Xue, G., Chen, J., Luo, J., Zhou, X., Gao, P. & Wang, Q. 2018 Oxidation of cefalexin by thermally activated persulfate: kinetics, products, and antibacterial activity change. *Journal of Hazardous Materials* **354**, 153–160.

Rajaei, F., Taheri, E., Hadi, S., Fatehizadeh, A., Amin, M. M., Rafei, N., Fadaei, S. & Aminabhavi, T. M. 2021 Enhanced removal of humic acid from aqueous solution by combined alternating current electrocoagulation and sulfate radical. *Environmental Pollution* **277**, 116632.

Song, H., Li, Q., Ye, Y., Pan, F., Zhang, D. & Xia, D. 2021 Degradation of cephalexin by persulfate activated with magnetic loofah biochar: performance and mechanism. *Separation and Purification Technology* **272**, 118971.

Tavasol, F., Tabatabaie, T., Ramavandi, B. & Amiri, F. 2020 Design a new photocatalyst of sea sediment/titanate to remove cephalexin antibiotic from aqueous media in the presence of sonication/ultraviolet/hydrogen peroxide: pathway and mechanism for degradation. *Ultrasonics Sonochemistry* **65**, 105062.

Tavasol, F., Tabatabaie, T., Ramavandi, B. & Amiri, F. 2021 Photocatalyst production from wasted sediment and quality improvement with titanium dioxide to remove cephalexin in the presence of hydrogen peroxide and ultrasonic waves: a cost-effective technique. *Chemosphere* **284**, 131337.

Ushani, U., Lu, X., Wang, J., Zhang, Z., Dai, J., Tan, Y., Wang, S., Li, W., Niu, C., Cai, T., Wang, N. & Zhen, G. 2020 Sulfate radicals-based advanced oxidation technology in various environmental remediation: a state-of-the–art review. *Chemical Engineering Journal* **402**, 126232.

Vieira, W. T., De Farias, M. B., Spaolonzi, M. P., Da Silva, M. G. C. & Vieira, M. G. A. 2021 Latest advanced oxidative processes applied for the removal of endocrine disruptors from aqueous media – A critical report. *Journal of Environmental Chemical Engineering* **9** (4), 105748.

Wang, S., Wu, J., Lu, X., Xu, W., Gong, Q., Ding, J., Dan, B. & Xie, P. 2019 Removal of acetaminophen in the Fe^{2+}/persulfate system: kinetic model and degradation pathways. *Chemical Engineering Journal* **358**, 1091–1100.

Wojnárovits, L. & Takács, E. 2019 Rate constants of sulfate radical anion reactions with organic molecules: a review. *Chemosphere* **220**, 1014–1032.

Yan, Z., Gu, Y., Wang, X., Hu, Y. & Li, X. 2021 Degradation of aniline by ferrous ions activated persulfate: impacts, mechanisms, and by-products. *Chemosphere* **268**, 129237.

Yang, Q., Ma, Y., Chen, F., Yao, F., Sun, J., Wang, S., Yi, K., Hou, L., Li, X. & Wang, D. 2019 Recent advances in photo-activated sulfate radical-advanced oxidation process (SR-AOP) for refractory organic pollutants removal in water. *Chemical Engineering Journal* **378**, 122–149.

Yu, L., Wang, L., Liu, Y., Sun, C., Zhao, Y., Hou, Z., Peng, H., Wang, S. & Wei, H. 2021 Pyrolyzed carbon derived from red soil as an efficient catalyst for cephalexin removal. *Chemosphere* **277**, 130339.

First received 21 August 2021; accepted in revised form 14 November 2021. Available online 29 November 2021